Chapter 1

Smoothing along geologic dip

INTRODUCTION AND SUMMARY

Velocity estimation is generally under-determined. To obtain a pleasing result we impose some type of regularization criteria such as preconditioning(Harlan, 1996), limiting inversion solutions to large singular values (Rowbotham and Pratt, 1997), or characterizing the model through a small number of spline coefficients (Ji, 1997). These methods all create velocity models that can correctly model the recorded travel times, but are often geologically unrealistic.

To create more geologically feasible velocity models and to speed up convergence, Michelena and Harris (1991) suggested using varying sized grid cells. Unfortunately, such a parameterization is prone to error when the wrong size blocks are chosen (Delprat-Jannaud and Lailly, 1992). Other authors have suggested locally clustering grid cells (Carrion, 1991) or characterizing the velocity model as a series of layers (Kosloff et al., 1996). These methods are also susceptible to errors when the wrong parameterization is chosen.

An attractive alternative approach is to add an additional model regularization term to the objective function (van Trier, 1990). In theory, this regularization term should be the inverse model covariance matrix (Tarantola, 1987) obtained from some *a priori* information sources.

For tomography, a geologist's structural model of the area, well log information, or preliminary stack or migration results all could provide useful information. Incorporating these varied information sources into the objective function is problematic. Geostatisticians have successfully combined these mixed types of information (Hirsche et al., 1997). Unfortunately, the geostatistical approach does not easily fit within a standard global tomography problem. More promising approaches were presented by Delprat-Jannaud and Lailly (1992) and Kaipio et al. (1999). Delprat-Jannaud and Lailly (1992) incorporated into the objective function a term encouraging the velocity gradient to follow reflector position. Kaipio et al. (1999) suggested using *a priori* structural information to create conditional covariance matrices.

In this chapter I take a different approach to adding geological dip information to velocity estimation. I start from the same basic assumption as Delprat-Jannaud and Lailly (1992); that velocity follows structural dip or some other known trend. Rather than minimizing the velocity gradient directly in the objective function I note that I can approximate a single dip by creating small plane wave annihilation filter (Claerbout, 1992a). By adjusting the shape and coefficients within this filter (which I refer to as a *dip penalty filter*), I can approximate a wide range of covariance responses. By building a space varying regularization operator out of these filters (a *steering filter*) I can approximate a model covariance which is space-variant. To speed up convergence I reformulate the regularization problem as a preconditioned problem (Claerbout, 1998a) using the helix transform and polynomial division (Claerbout, 1998b).

I will begin by introducing a simple missing data problem. I show how the geophysicist and geostatistician find different ways to characterize and incorporate the model covariance function into an inverse problem. One geophysics approach, applying a Prediction Error Filter (PEF), can often obtain a better image. The downside of the PEF approach is it requires having a field with the same statistical properties as the variable we are attempting to estimate. I then introduce another way to characterize the model covariance function, dip penalty filters, that combines the geostatistician's ability to use disparate and irregular information sources and the geophysicist's ability to solve complex inversion problems. I go on to describe how to find dip penalty filter directions and how to build a steering filter. I show how to speed up convergence by reformulating problems in terms of preconditioning rather than regularization. I conclude the chapter by showing that a steering filter improves the tomography estimate using

the synthetic introduced in Chapter **??**.

WHY REGULARIZE?

In general, geophysical inverse problems (inverting for some model **m**, given some **d**, while applying some operator **L**) are ill-posed. A classic example of this is the missing data problem (Claerbout, 1998a; Isaaks and Srivastava, 1989). The goal of the missing data problem is to interpolate intelligently between a sparse set of known points. For example, let us take a synthetic velocity model with an upper horizontal reflector, an anticline between two unconformities, and updipping layer at the bottom of the model. Suppose we have velocity measurements at several wells and you would like to interpolate it onto a regular 2-D mesh, Figure 1.1.

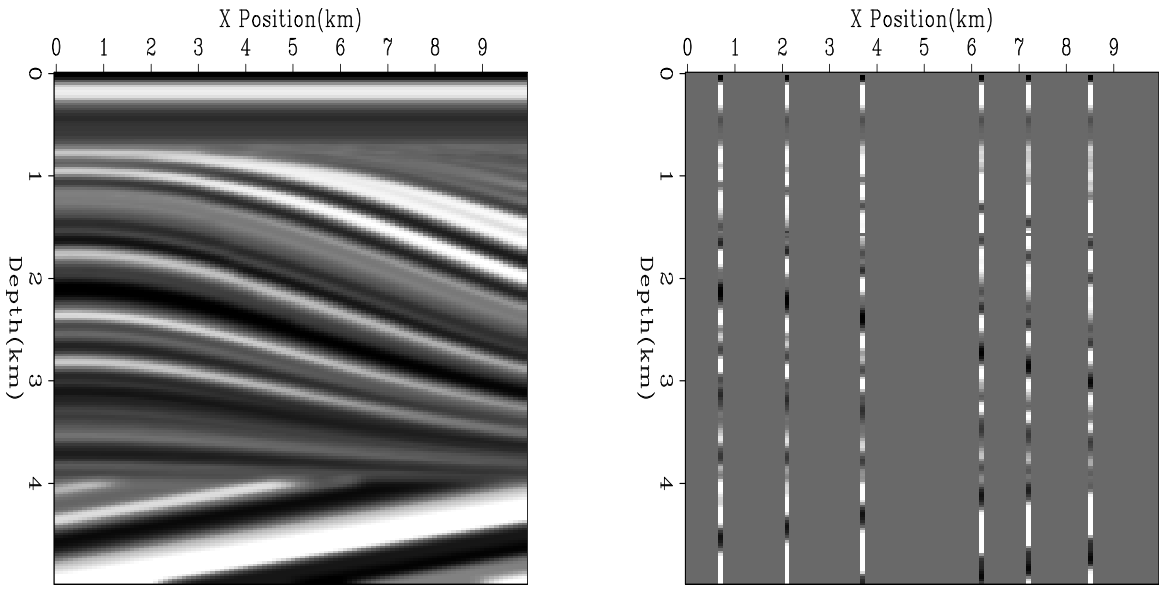

Figure 1.1: Left panel shows a synthetic velocity model, right panel shows a subset of that data chosen to simulate well log data. steer-well-logs [ER]

The geophysicist might follow the approach described by Claerbout (1998a), first interpolating the irregular data onto a regular mesh by applying some type of binning operator, **B**,

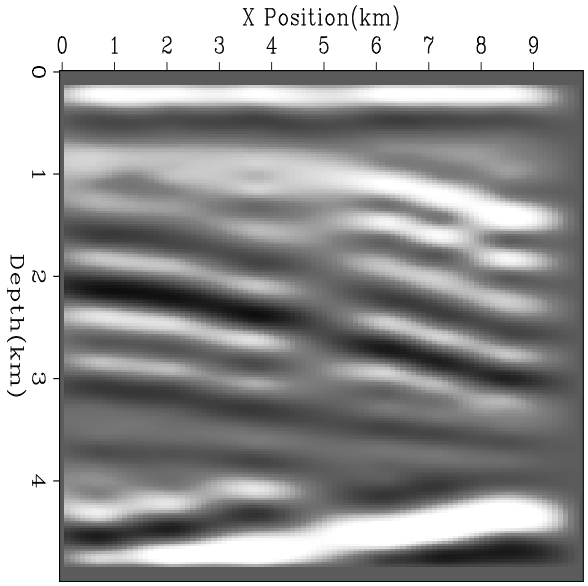

Figure 1.2: Interpolation result after 200 iterations using an inverse Laplacian regularization operator. Note the edges effects at the top and bottom of the model due to using an internal convolution operator. steer-qdome-lap [ER,M]

then defining a fitting goal that requires the model to fit the data exactly at the known points **J**.

$$\mathbf{JBd} \approx \mathbf{Jm}. \tag{1.1}$$

At model locations where there are no data values we want the model to be 'smooth', therefore we will use Tikhonov regularization(Tikhonov and Arsenin, 1977) to minimize the output of a roughening operator applied to the model,

$$\mathbf{0} \approx \mathbf{Am}. \tag{1.2}$$

For the remainder of the thesis I will refer to (1.2) as the *model styling* goal.

If we don't have any other knowledge about the model, an isotropic operator like the Laplacian might be a logical choice for **A**. If I apply the fitting goals implied by (1.1) and (1.2) for 200 iterations using the Laplacian for **A**, I get Figure 1.2. The result is what has been euphemistically referred to as the 'ice cream cone result' (Brown, 1998). By spreading information isotropically the model goes smoothly from the known points to some local average. We see little to no continuation of layers, generally a thoroughly unsatisfactory result.

APPROXIMATING THE COVARIANCE MATRIX

With no other information the Laplacian might be the best regularization operator that we could use. But if we know something else about out model, can we do better? According to Bayes theory we should be using the inverse model covariance for the regularization operator. Unfortunately the model covariance matrix is not generally obtainable. If the model covariance matrix is unreasonable to estimate and use, what is a more reasonable goal?

All statistical measures have underlying assumption of repetition. The model only has a single value at each location, as a result common practice is to use nearby points to simulate repetition. By using multiple points we are making an assumption of stationarity. The definition of stationarity for a random process is that the joint distribution of any two points does not depend on their location just the vector distance **x**.

If we accept the stationarity assumption there are several related ways that we can characterize the relationship between nearby points. If we transform our model into the frequency domain $M(k)$ we can calculate the model's spectrum $S(k)$:

$$S(k) = \overline{M}(k)M(k). \tag{1.3}$$

We can obtain an equivalent measure in the space domain by calculating a model's autocorrelation. The covariance $C(\mathbf{x})$ is just the autocorrelation with the mean subtracted,

$$C(\mathbf{x}) = < m_i - \hat{m}_i > - < m_j - \hat{m}_j >, \tag{1.4}$$

where

$<>$ is an ensemble average.

m_i **and** m_j are points separted by the distance **x**.

$\hat{m}_i$ **and** $\hat{m}_j$ are the average values.

Figure 1.3 shows the result of applying equation (1.4) to the left panel of Figure 1.1. In the

next subsections I will show how geophysicists and geostatisticians use these related measures to solve the missing data problem.

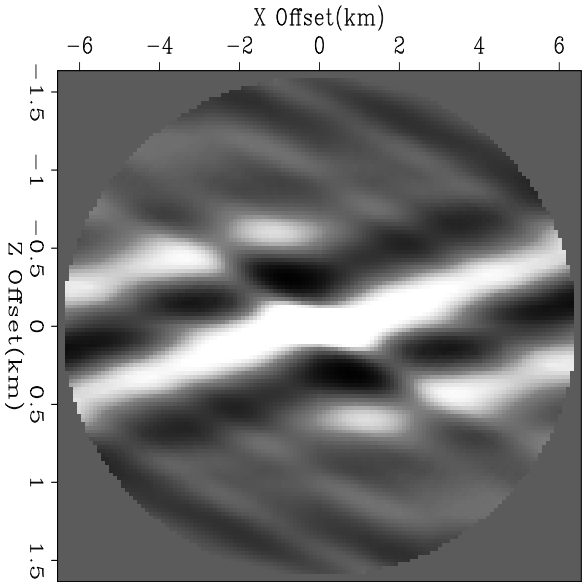

Figure 1.3: Spatial covariance matrix for the velocity model in Figure 1.1. Note that the dip below the lower unconformity dominates the covariance calculation. steer-model-covar [ER]

Geophysical approach

A standard approach at SEP, and to a limited extent the geophysical community at large, is to characterize the model covariance through a Prediction Error Filter (PEF). The geophysicist notes that if we solve

$$\mathbf{Ma} \approx \mathbf{0}, \tag{1.5}$$

where **M** is convolution with a field that has the same properties as the model, and **a** is the PEF, the output of this convolution is white (Claerbout, 1992a). Therefore **a** must have the inverse spectrum of the model. This is only true if we have chosen a sufficient shape and size for **a**. By changing the shape of **a** we can control how many and which dips of the model we see. If we construct **a** to find dips at all possible angles and then apply (1.5) we get Figure 1.4 as the impulse response of the filter. The PEF captured the prominent dip going up at approximately 15 degrees and also a minor dip going down at approximately 30 degrees. The right panel of Figure 1.4 shows the result of applying the PEF to the missing data problem. We have done a substantially better job filling in the missing data compared to the Laplacian result, Figure 1.2,

but its still far from ideal. The filter has introduced both dips at every location and as a result we have a model that is unreasonable.

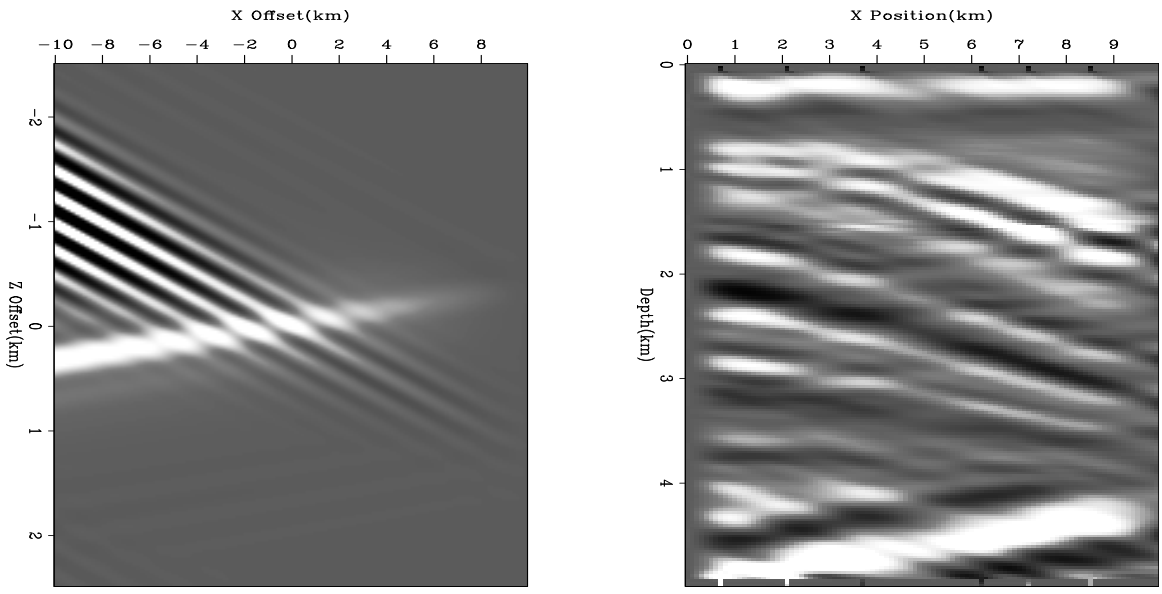

Figure 1.4: The left panel shows the impulse response of the PEF found from the velocity field (left panel of Figure 1.1). The right panel shows the result of applying the PEF to the missing data problem (the input being the right side of Figure 1.1). steer-gp-mis [ER]

Geostatistical approach

The geostatistician takes another approach, called kriging. Instead of solving a global optimization problem the geostatistician solves a series of small inversion problems. They assume that the model point $m(\mathbf{u})$ (where $\mathbf{u}$ is its location in the vector space) is a linear combination of n nearby data points $d(\mathbf{u_1})...d(\mathbf{u_n})$,

$$m(\mathbf{u}) = \sum_{\alpha=1}^{\mathbf{n}} \lambda_\alpha(\mathbf{u}) \mathbf{d}_\alpha . \tag{1.6}$$

The weights λ_α are calculated to minimize the error variance and result in the set of equations,

$$\begin{bmatrix} C(\mathbf{u_1}-\mathbf{u_1}) & \dots & C(\mathbf{u_n}-\mathbf{u_1}) & 1 \\ . & \dots & . & . \\ . & \dots & . & . \\ . & \dots & . & . \\ C(\mathbf{u_1}-\mathbf{u_n}) & \dots & C(\mathbf{u_n}-\mathbf{u_n}) & 1 \\ 1 & \dots & 1 & 0 \end{bmatrix} \begin{bmatrix} \lambda_1 \\ . \\ . \\ . \\ \lambda_n \\ \mu \end{bmatrix} = \begin{bmatrix} C(\mathbf{u}-\mathbf{u_1}) \\ . \\ . \\ . \\ C(\mathbf{u}-\mathbf{u_n}) \\ 1 \end{bmatrix}. \tag{1.7}$$

Each $C(\mathbf{x})$ is taken from a predefined covariance estimate (Figure 1.5). To guarantee that the matrix in equation (1.7) is positive definite the geostatisticians approximate the covariance function through a linear combination of a limited set of functions. Each function is described by:

range, the distance at which the covariance function is essentially gone to 0,

anisotropy, the amount the covariance function depends on radial angle, and

orientation, the major orientation axis of the covariance function.

These parameters are used to describe a spherical, exponential, Gaussian, or power model that are guaranteed to produce a positive definite covariance matrix.

The left panel of Figure 1.6 shows the geostatistical approximation of the model covariance for the missing data problem. This approximation does a good job characterizing the primary dip of the covariance function, but does not accurately describe the *range* of the covariance function. The right panel of Figure 1.6 shows the result of applying kriging to the same missing data problem. The result is fairly comparable to the geophysics result. Instead of adding a second dip at every location we have only forced the primary dip. Because this approximation adds insufficient *range* for the covariance function the answer returns to the local average between the two wells with the greatest separation. Overall the result is as unsatisfactory as the geophysics approach to the problem.

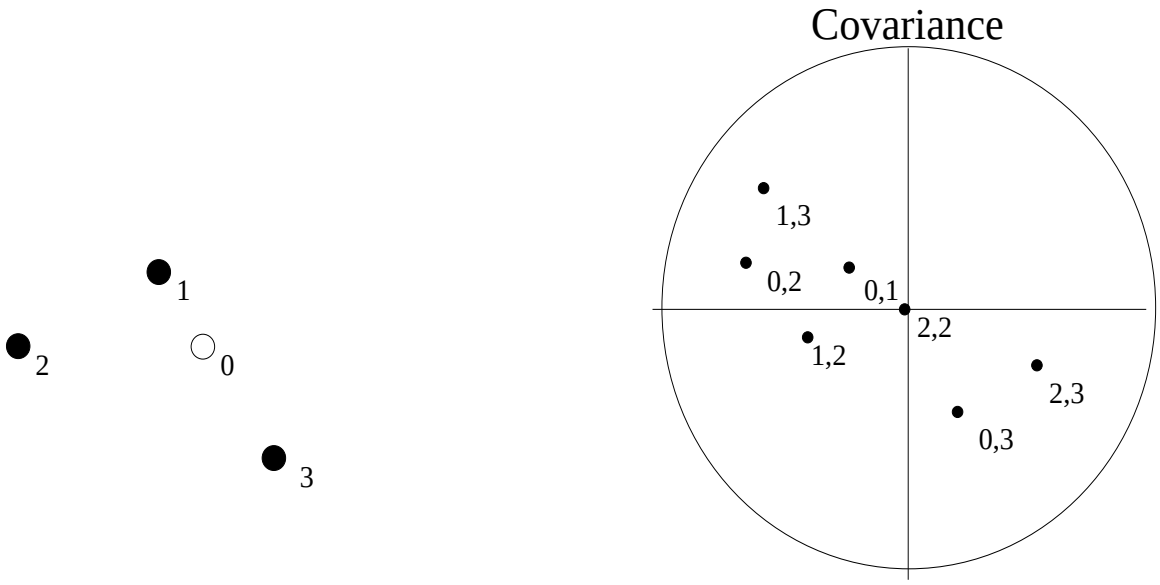

Figure 1.5: Definition of the terms in equation (1.7). A vector is drawn between two points. The covariance at the angle and distance describing the vector is then selected. steer-covar-def [NR]

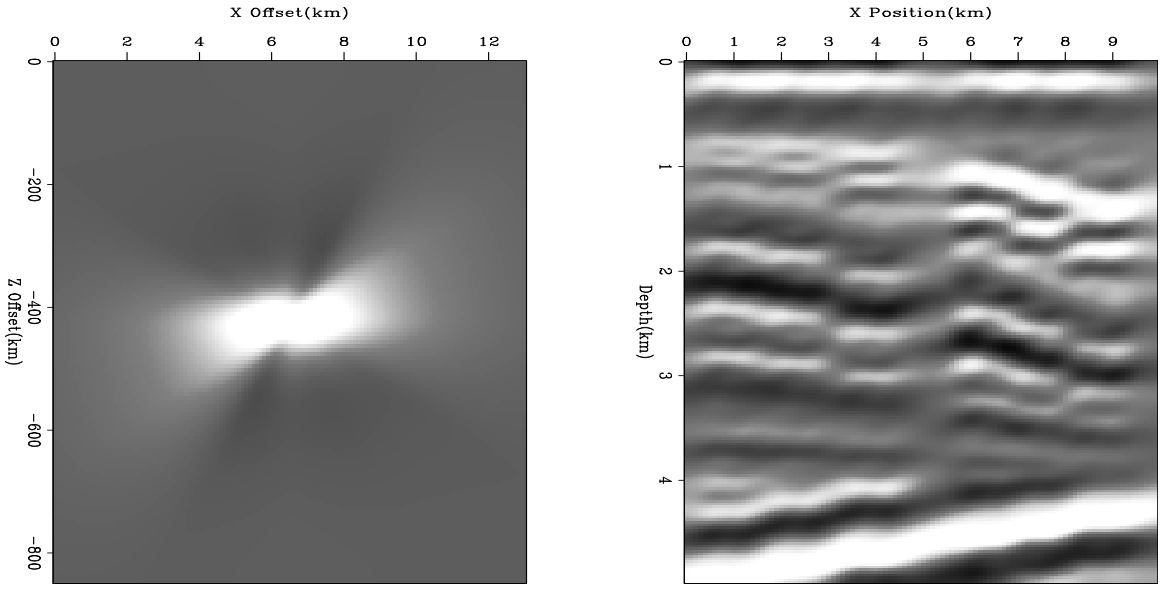

Figure 1.6: Left panel shows the approximated covariance matrix, right panel is the result of solving equation (1.7) at every unknown model point. steer-geostat-mis [ER]

STATIONARITY

Both the geostatistical and geophysical approach give poor results because we are ignoring a basic tenet that both methods are built on: stationarity. An underlying assumption of both methods is that the statistics of the data do not vary with location. If we look at the covariance at four different regions in the data, Figure 1.7, we can see that covariance changes dramatically throughout the model. The top left covariance is taken from the flat structure at the top of the model, and shows a strong horizontal trend. The top right represents the covariance along the upper portion of the anticline and has a slight dip down to the right. The bottom left is the covariance from the lower portion of the anticline and captures the sharper dip down-right in the region. The final panel, the bottom-right represents the area below the unconformity and captures the up-dipping structure.

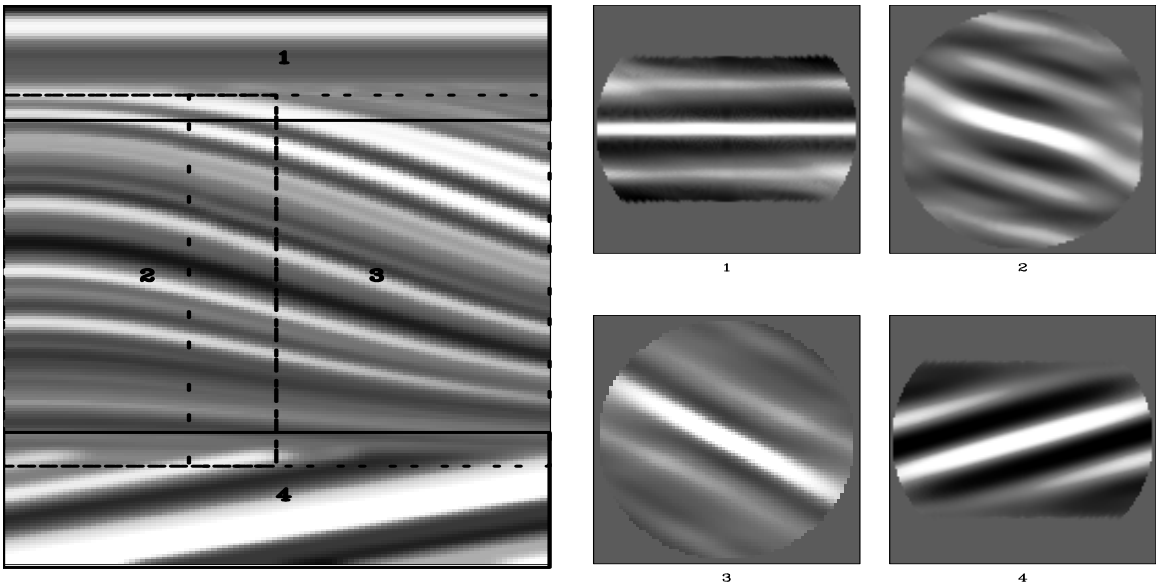

Figure 1.7: The covariance at four different regions of the model (left panel of Figure 1.1). The top left is above the upper unconformity; top right, the upper portion of the anticline; bottom left, lower portion of the anticline; and bottom right, below the lower anticline. steer-covar-change [ER]

Patching

A common solution to this non-stationarity is to break the problem into patches (geophysics terminology) (Claerbout, 1992b) or ‘distinct sub zones’ (geostatistics terminology). We define regions where the assumption of stationarity is valid, and apply the given technique in the region. We then recombine the sub-regions into the final model. Figure 1.8 shows the result of defining the model space into the four different regions of Figure 1.7 and then applying the geophysical and geostatistical approach. Note that the image is significantly improved over the single covariance function approach. The *range* description for the geostatistical approach is poor, the images are still of significantly lower frequency than the known model (multiple realizations, a geophysics equivalent of which is presented in Appendix **??**, can provide a higher frequency answer), and we still haven’t done a very good job within the anticline.

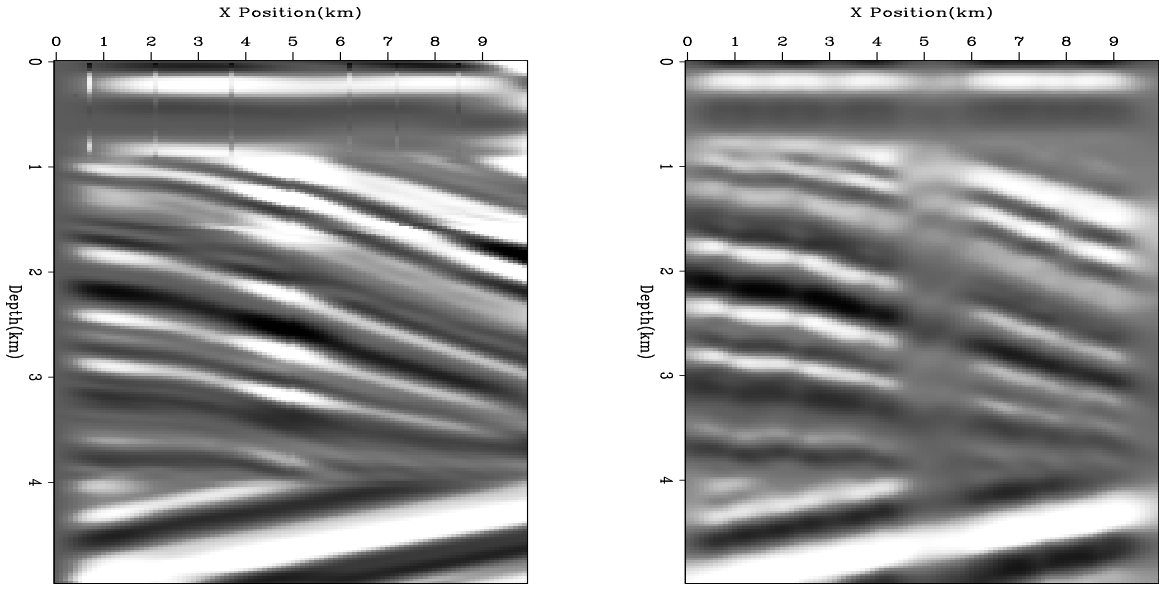

Figure 1.8: The result of breaking the problem into four patches and solving them independently. Left panel is the result of applying the geophysical method, the right geostatistics. steer-patch [ER,M]

STEERING FILTER

If we reexamine the desired velocity function it is apparent that the covariance function varies within at least two of the four patches (we can also see this in the covariance function of patch 2 and 4 of Figure 1.7). Therefore, it follows that we should get a better image by making smaller and smaller patches. Crawley (1998) showed that this is true when solving a data interpolation problem. Unfortunately, we can only make the patch size so small before we can't generate sufficient statistics to find the PEF or solve the kriging equations. In addition, the geophysical solution relies on having a field with the same statistical properties as the model, this is often not the case. Often what we have is what geostatisticians refer to as 'soft data'. Soft data has *generally* the same properties of the variable of interest but it is often in incompatible form, a classic example of this is tying well measurements to flow simulation results. Geostatistics is generally better suited for combining mixed and limited data. Kriging requires us to provide only a variogram for each sub-zone. On the other hand, the geostatistical approach is not well suited for fitting into an iterative optimization problem. Kriging wants the physics of the problem to be describable by a known function that would then form the basis for a space varying mean for the kriging problem (Isaaks and Srivastava, 1989). For problems like tomography this is an unacceptable requirement.

In geophysics there have been attempts to combine different information sources (Stork, 1994),but with limited success. Generally, the inversion problems are too large to use classical hard constraint mechanisms (Polak, 1997). What we need is a method to construct a space-varying filter that does a good job describing the model covariance, but can be obtained from limited and disparate information sources.

If we look at regions two and four in Figure 1.7 we can see that when the stationary assumption is valid the covariance matrix is fairly simple. We have a primary trend oriented along the dip of the velocity field that slowly dies out and a ringing effect due to the sinusoidal nature of the model. We would like to come up with a way to emulate the primary trend of the covariance matrix through minimal information.

To do this it is important to remember that the regularization operator should have the inverse spectrum of the covariance matrix. Therefore if the covariance function is primarily

a dipping event, the regularization operator should be destroying that dip. Claerbout (1990; 1992a) showed how to estimate the primary dip in a region and how to construct a filter that could destroy that dip. These small filters, which I refer to as *dip penalty filters*, can be as simple as a two or three point filter, Figure 1.9. A dip penalty filter consists of a fixed '1' and one or more coefficients in the next column. The location of the filter coefficients in the second column determines the dip that the filter will destroy. Figure 1.10 is the inverse impulse response of Figure 1.9. Note how the general orientation of the impulse response is approximately the same as the covariance function below the lower unconformity, but the *anisotropy* and *range* are not correct. In the next section I will discuss how we can also control these parameters with dip penalty filters.

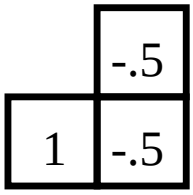

Figure 1.9: A dip penalty filter oriented approximately 22.5 degrees. steer-small-filter [NR]

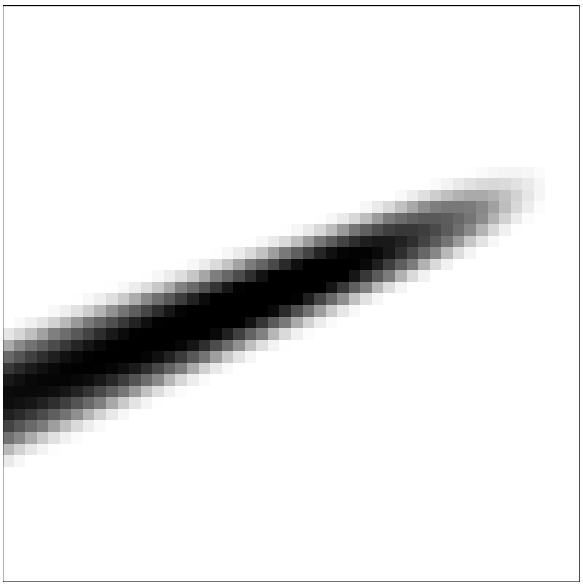

Figure 1.10: The result of applying $\frac{1}{\mathbf{A}\mathbf{A}'}$ where **A** is the filter in Figure 1.9. steer-small-response [ER]

Constructing a filter

When building a steering filter, we want to create a filter that destroys a given slope p. Further, we would like to control the bandwidth response of filters oriented at different slopes. We can achieve both these goals by constructing a simple filter. The filter will have a one at the zero lag location and the rest of its values one column away. For determining the non-zero lag values imagine constructing a triangle whose center is located at the desired slope p. The width w of the triangle determines the size of the filter (only coefficients within the triangle will be used) and the filter's level of *anisotropy*. The height of the filter a determines the *range* over which the filter will operate. We can express the values of the filter by,

$$f(x) = -a \frac{\left(\frac{w}{2} - |x| - p\right)}{\frac{w}{2} \sum_{\text{lag}} f(x)}, \tag{1.8}$$

where x is the vertical distance away from the zero lag coefficient.

For example, let's return to the missing data problem. If we limit the *a priori* information to the assumption that velocity follows structure and we have some guesses at reflector position, we can use this information to build a complex operator (which I will refer to as a *steering filter*) composed of dip penalty filters. For this problem we will assume that we have the location of four reflectors, one above the top unconformity, two between the unconformities and one below the lower unconformity (left-panel of Figure 1.11). If we interpolate these dips to the entire model space we have all we need to construct a steering filter operator. If we use this operator as the regularizer we get Figure 1.12 as the interpolation result. The steering filter did a significantly better job than the patching approach. With more information about the model (more reflectors, an idea on the level of *anisotropy* in different portions of the model, etc.) we could do even better by using some of the other adjustable parameters available when constructing the steering filter operator.

The three adjustable parameters, possibly different at every model point, in the filter construction can seem daunting but is what enables almost any covariance function to be described by steering filters. In certain regions of the model you might feel that that covariance function is much more isotropic. In these regions you could consider making your triangle bigger to

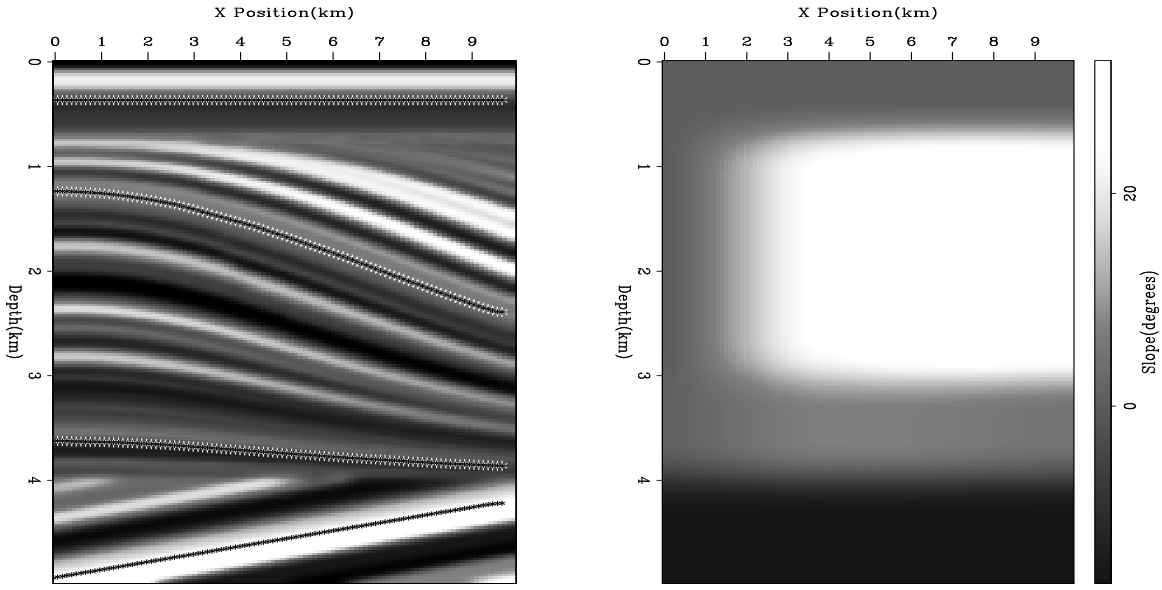

Figure 1.11: Left panel are four reflectors chosen to represent the *a priori* information. The right panel is interpolated slope calculated from the reflectors that will form the basis of the dip penalty filter. steer-qdome-refs [ER]

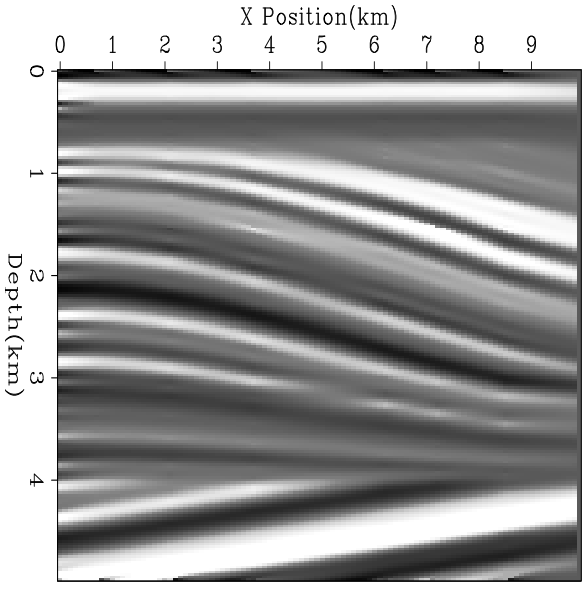

Figure 1.12: The result of using the steering filter operator as regularizer to the missing data problem. steer-qdome-reg-cont [ER,M]

smooth your filter coefficients over a wider angle *range*, while keeping it small in areas where the covariance is much more *anisotropic*. The sum of the non-zero lag coefficients opens up another intriguing freedom. As Figure 1.14 shows, when the sum of the non-zero lag coefficients gets close to -1, the area over which the smoother operates increases greatly. This is similar to increasing the ϵ value over only a portion of your model space. This enables steering filters to handle a model space where the *range* difference is variable. The final parameter we can vary, p, controls the angle at which we wish to smooth (Figure 1.15). Note how imposing a triangle has helped, but not completely eliminated, the variance in angular bandwidth response of the filter (Figure 1.13).

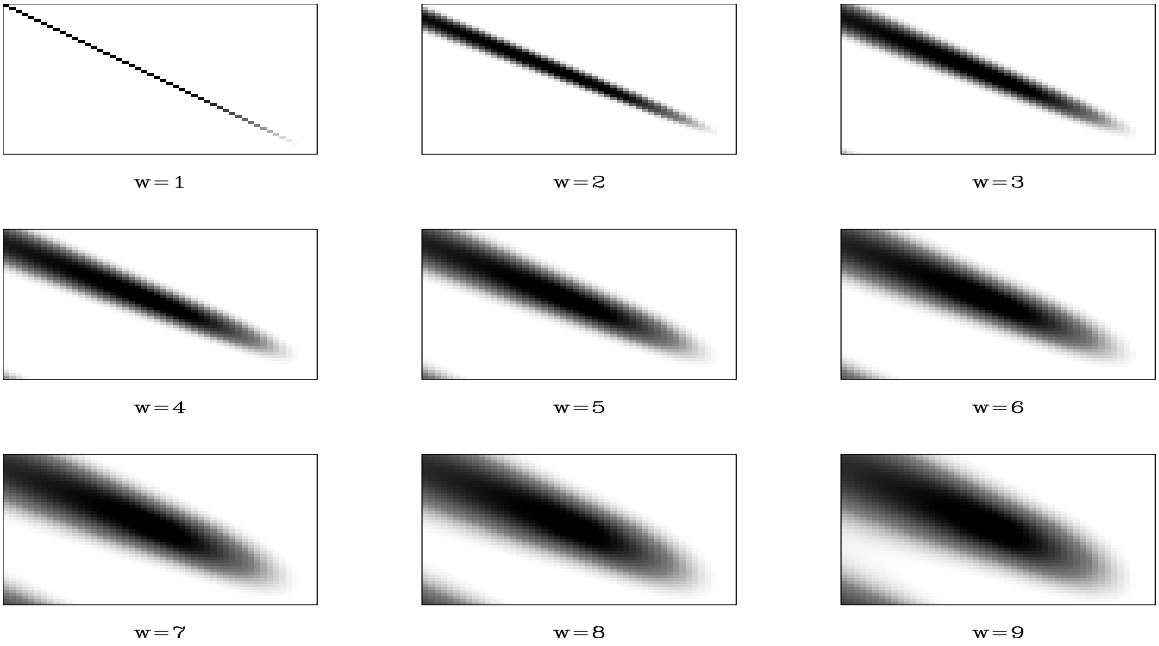

Figure 1.13: The impulse response of the smoothing filter as function of the triangle base. Note the wider the base, the less precise the dip smoothing. steer-width [ER,M]

REGULARIZING VS. PRECONDITIONING

An important consideration in many geophysical problems, including tomography, is speed of convergence. Tomography, even ray based, is computationally intensive so it is important to minimize the number of steps it takes to get to a reasonable solution. One of the reasons

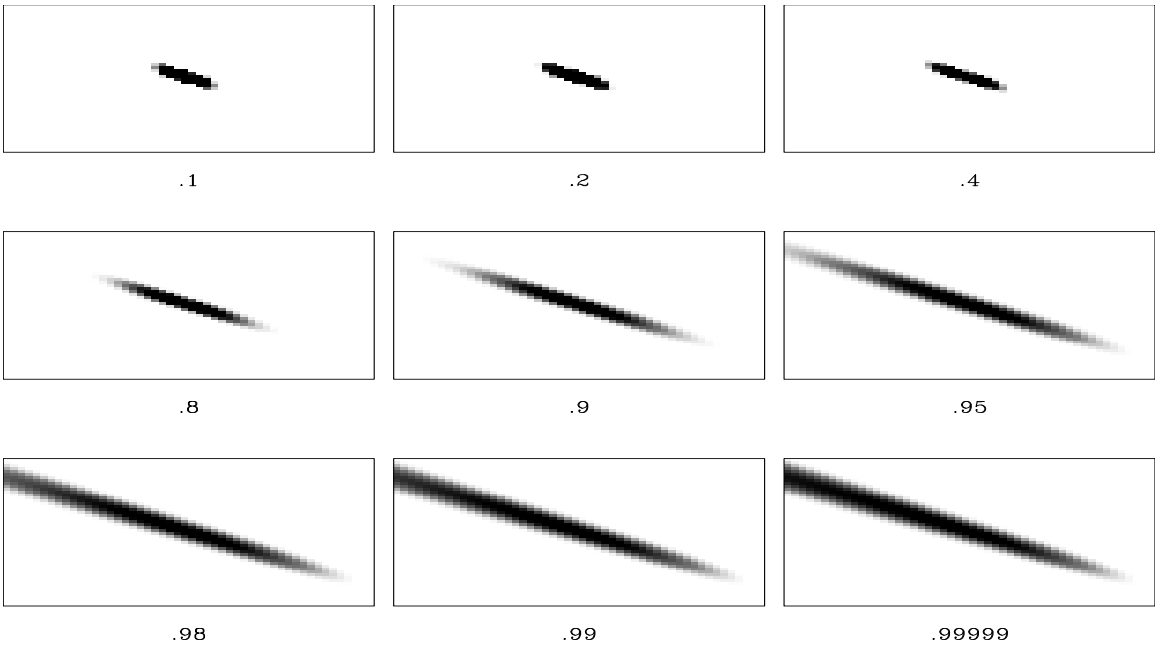

Figure 1.14: The impulse response of the smoothing filter as the sum of the non-zero lag coefficients get closer too 1. steer-distance [ER,M]

for slow convergence is that the regularization operators, including steering filters, are small in size. As a result the condition number of the matrix we are attempting to invert is large. A classic solution is to reformulate the regularized inversion problem into a preconditioned problem in terms of some new variable $\mathbf{p}$ (Polak, 1997) and used in tomography by Harlan (1995). The goal is to replace the regularization operator $\mathbf{A}$ with a preconditioning operator $\mathbf{B}$ that smooths long distances with each iteration. Any smoother could be an effective preconditioning operator but the ideal choice for $\mathbf{B}$ would be $\mathbf{A^{-1}}$, because if $\mathbf{B} = \mathbf{A^{-1}}$, the regularized fitting goals (1.1) and (1.2) would be equivalent to the new preconditioned fitting goals (Fomel et al., 1997),

$$\begin{aligned} \mathbf{d} &\approx \mathbf{L}\mathbf{A}^{-1}\mathbf{p} \\ \mathbf{0} &\approx \mathbf{A}\mathbf{m} = \mathbf{A}\mathbf{A}^{-1}\mathbf{p} = \mathbf{I}\mathbf{p}. \end{aligned} \tag{1.9}$$

The speed up is due not only to the preconditioner spreading information long distances with every iteration but also to the regularization equation now being the identity matrix. The

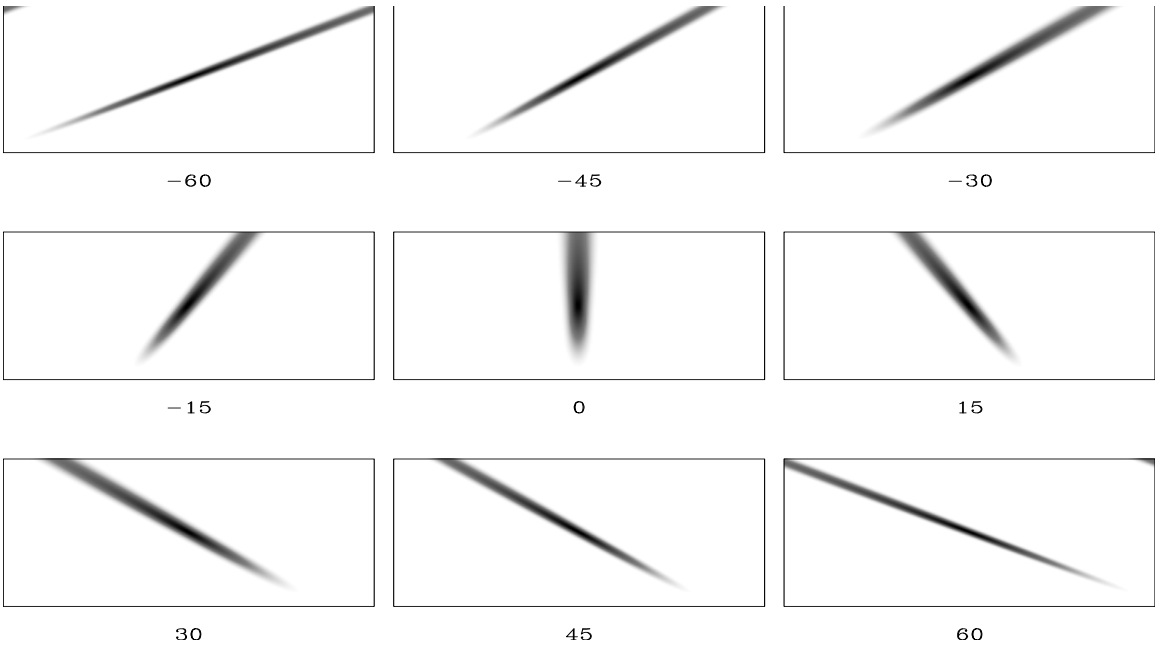

Figure 1.15: The impulse response as we vary angle. Note how the bandwidth response varies slightly with angle. Note the helix wrap-around in the top-left and bottom-right plots. steer-angle [ER,M]

identity matrix is its own inverse therefore reducing the condition number of the matrix we are trying to invert.

Helix transform

The problem with this approach is that the regularization operator is multi-dimensional. Inverting the operator requires a trick that has only been recently been used in geophysics (Claerbout, 1998b). Given a multi-dimensional filter, such as Figure 1.9, you first map it onto the coordinate space of the data (panel *a* of Figure 1.16). Then imagine wrapping the data around a cylinder with the end of column one connected the beginning of column two. Finally, unwind the data into a single string of numbers and you have converted your multi-dimensional filter into a 1-D filter! If this new, one-dimensional filter is causal and minimum phase, which steering filters are, you can apply the inverse of the filter cheaply through polynomial division (Claerbout, 1976).

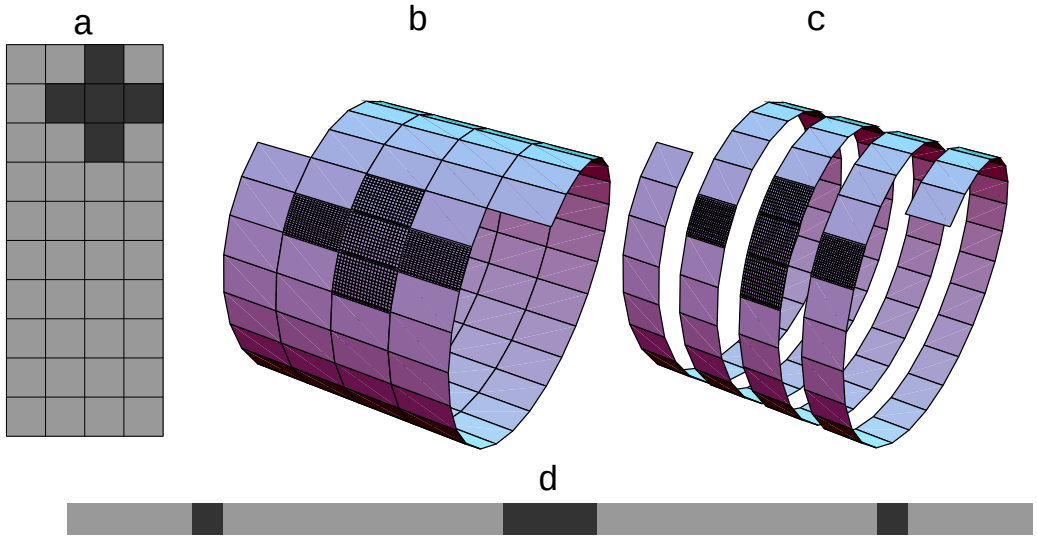

Figure 1.16: Filtering on a helix. The same filter coefficients overlay the same data values if the 2-D coils are unwound into 1-D strips. This figure was taken from Fomel and Claerbout (1997). steer-helix [NR]

With the helix we can now solve the missing data problem that took us 40 iterations as a

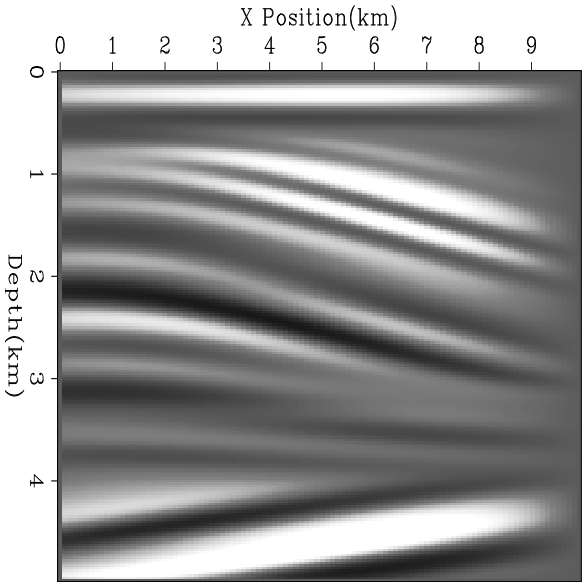

Figure 1.17: The interpolation result after six iterations using the preconditioned formulation (1.10) of the problem. steer-qdome-prec-cont [ER,M]

regularized problem, Figure 1.12, in six iterations at the same cost per iteration with the same quality result.

REGULARIZING TOMOGRAPHY

Finding smoothing directions

To build the steering filter operator we need a dip field, the range, and the level of anisotropy throughout the model. In many cases it is important to have all three of these parameters vary spatially. For this simple example, we are going to assign a constant *range* and *anisotropy* to the entire model. We will use the model introduced in chapter **??** (Figure **??**). For the dip field estimate we will assume that velocity follows dip and use the position in which the reflectors image at zero ray parameter. Figure 1.18 shows the dip directions based on the migrated reflector positions using the initial velocity estimate.

In depth the initial reflection positions are, of course, in error, so the dip field estimate is also flawed. Figure 1.19 shows the initial, correct dip field, and the error in the estimate. In the tau domain, where reflector positions are less effected by our velocity estimate, the dip

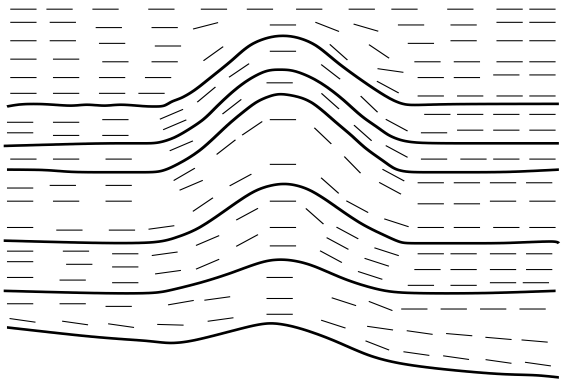

Figure 1.18: Steering filter directions as a function of geologic dip. The bold, solid lines are estimated reflector positions (taken from the initial migration), the remaining lines represent dip bars estimated by interpolating the dips between the reflectors. steer-dir [NR]

field estimate is better, and the steering filters (and therefore the characterization of the model covariance matrix) are more accurate (Figure 1.20).

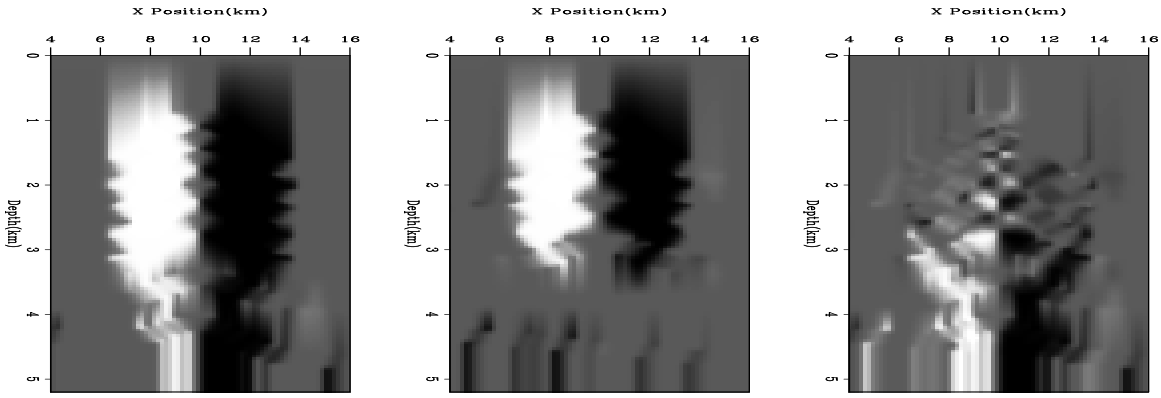

Figure 1.19: Left panel is the initial dip directions in depth. The center panel is the correct dip field generated from the known reflector positions. The right panel is the difference between the correct dip field and the estimated dip field. In each case the dip field is calculated by interpolating between the reflector above and below the given point. Below the bottom reflector dips are simply continued. The large error in the lower portion of the difference panel is due to the difference between the estimate, a bowing up of the bottom two reflectors, and their true geometry. steer-dips-z [ER,M]

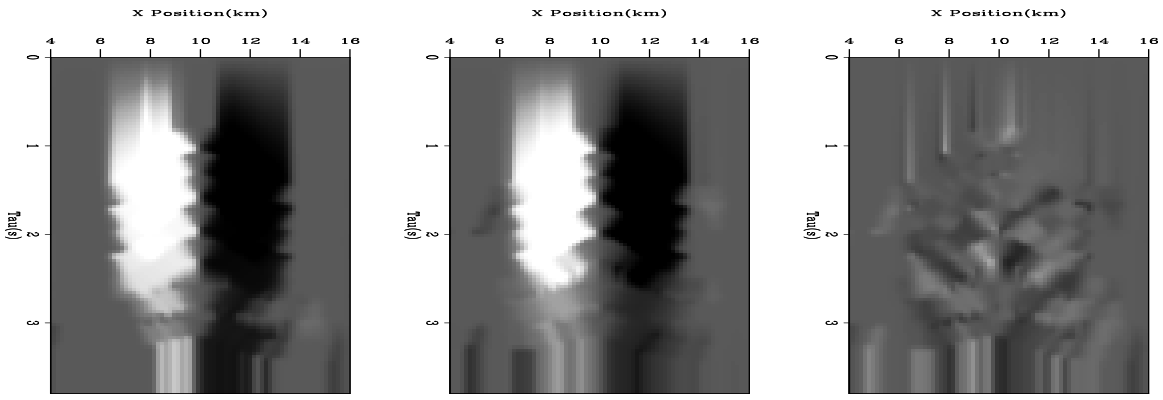

Figure 1.20: Left panel is the estimated dip field in the tau domain. The center panel is the correct dip field in the tau domain. The right panel is the initial error in the dip field estimate. Note that the dip estimate is significantly more accurate in the tau domain compared to the depth domain (Figure 1.19). steer-tau-dips [ER,M]

Fitting goals

Finally, we need to set up the tomography fitting goals in a preconditioned form. If we follow the same procedure as we did for the missing data problem, we would first add the regularization goal to the tomography problem:

$$\begin{aligned} \Delta \mathbf{t} &\approx \left(\mathbf{T}_{\tau,\mathbf{ref}} - \mathbf{T}_{\tau,\mathbf{ray}}\right) \Delta \mathbf{s} \\ \mathbf{0} &\approx \epsilon \mathbf{A} \Delta \mathbf{s}, \end{aligned} \tag{1.10}$$

where ($\mathbf{A}$) is the steering filter operator.

However, these fitting goals don't accurately describe what we really want. The steering filters are based on the desired slowness rather than change of slowness. With this fact in mind, we can rewrite the model styling goal as

$$\mathbf{0} \approx \epsilon \mathbf{A}(\mathbf{s_0} + \Delta \mathbf{s}), \tag{1.11}$$

or alternately as

$$-\epsilon \mathbf{A} \mathbf{s_0} \approx \epsilon \mathbf{A} \Delta \mathbf{s}. \tag{1.12}$$

Here we see the advantage of the helix. Without having the exact inverse of **A** as our preconditioner we would not be able to do the same substitution. The left hand side of the model styling goal is not equal to zero but we can still do the same preconditioning substitution:

$$\begin{aligned} \Delta \mathbf{t} &\approx \left(\mathbf{T}_{\tau,\mathbf{ref}} - \mathbf{T}_{\tau,\mathbf{ray}}\right) \mathbf{A}^{-1} \mathbf{p} \\ -\epsilon \mathbf{A} \mathbf{s_0} &\approx \epsilon \mathbf{I} \mathbf{p}. \end{aligned} \tag{1.13}$$

SYNTHETIC COMPARISONS

In this chapter I introduced the concept of approximating the covariance matrix through a non-stationary steering filter. When we add in the tau-versus-depth tomography of Chapter **??** we have four possible tomography schemes to compare. The four combinations I will refer to using the following shorthand:

depth-laplacian - Tomography in depth, smoothing the slowness field (compared to the change in slowness smoothing of Chapter **??**) with an isotropic smoother.

tau-laplacian - Tomography in the tau domain, smoothing slowness with an isotropic smoother.

depth-steering - Tomography in the depth domain, using steering filter smoothing.

tau-steering - Tomography in the tau domain, using steering filter smoothing.

For the comparison I will use the same data and initial model as used Chapter **??**. I will show the resulting velocity model and migration after one and after two non-linear iterations of each tomography method.

First iteration

Figure 1.23 shows the velocity model after one non-linear iteration of all four methods. Smoothing the slowness (*depth-laplacian* and *tau-laplacian*) rather than the change in slowness (Figure **??** of Chapter **??**) creates a more reasonable velocity model. This is most apparent when

looking at the low velocity layer. When smoothing the slowness we have added significantly more energy into the low velocity layer within the anticline structure. In addition we do not see the velocity reversal below the center of the anticline that we saw when smoothing the change in slowness. The resulting migration images, Figures 1.21 and 1.22, do not show similar improvement (when compared to Figures **??** and **??**). In this case we have been hurt by our choice of regularization operator. Our regularization operator will tend to create Gaussian blobs. The change in slowness that we need to introduce to our model is more accurately described by a Gaussian shape than the velocity is.

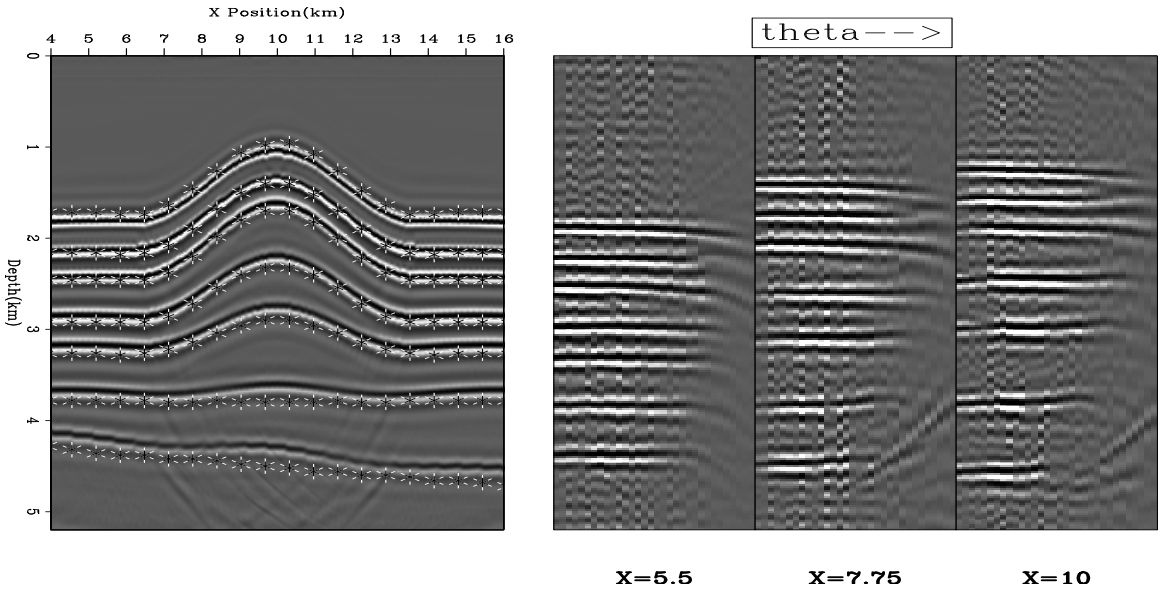

Figure 1.21: The migration result after one iteration of *depth-laplacian* steer-res.vel1.lapz [ER,M]

If we replace the isotropic regularizer with a steering filter the results improve significantly. In the *depth-steering* and *tau-steering* case the anticline structure is very evident. The low velocity layer also does a good job following the anticline. The migration results Figures 1.24 and 1.25 are both impressive. Both results have done a good job flattening the horizontal and dipping reflectors and show little residual moveout in the CRP gathers. The tau result does a better job correctly positioning the reflectors. Here we clearly see the advantage of the tau domain's ability to uncouple the focusing and mapping. In addition to reducing the map migration term in the tomography operator, we are able to correctly estimate the dip field for

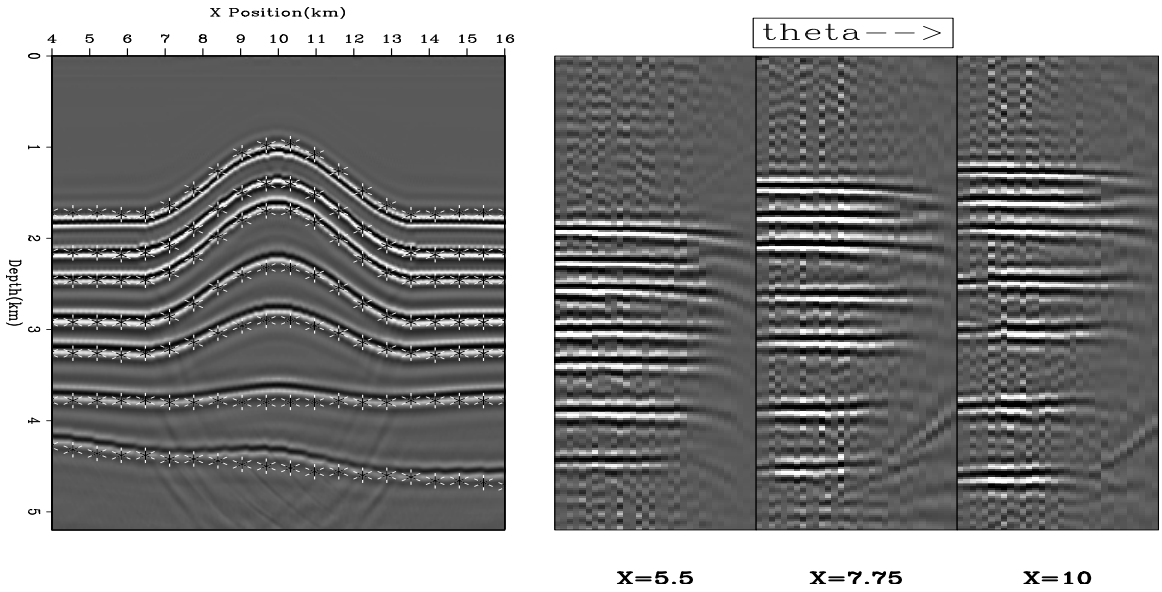

Figure 1.22: The migration result after one iteration of *tau-laplacian* steer-res.vel1.tau [ER,M]

the steering field operator.

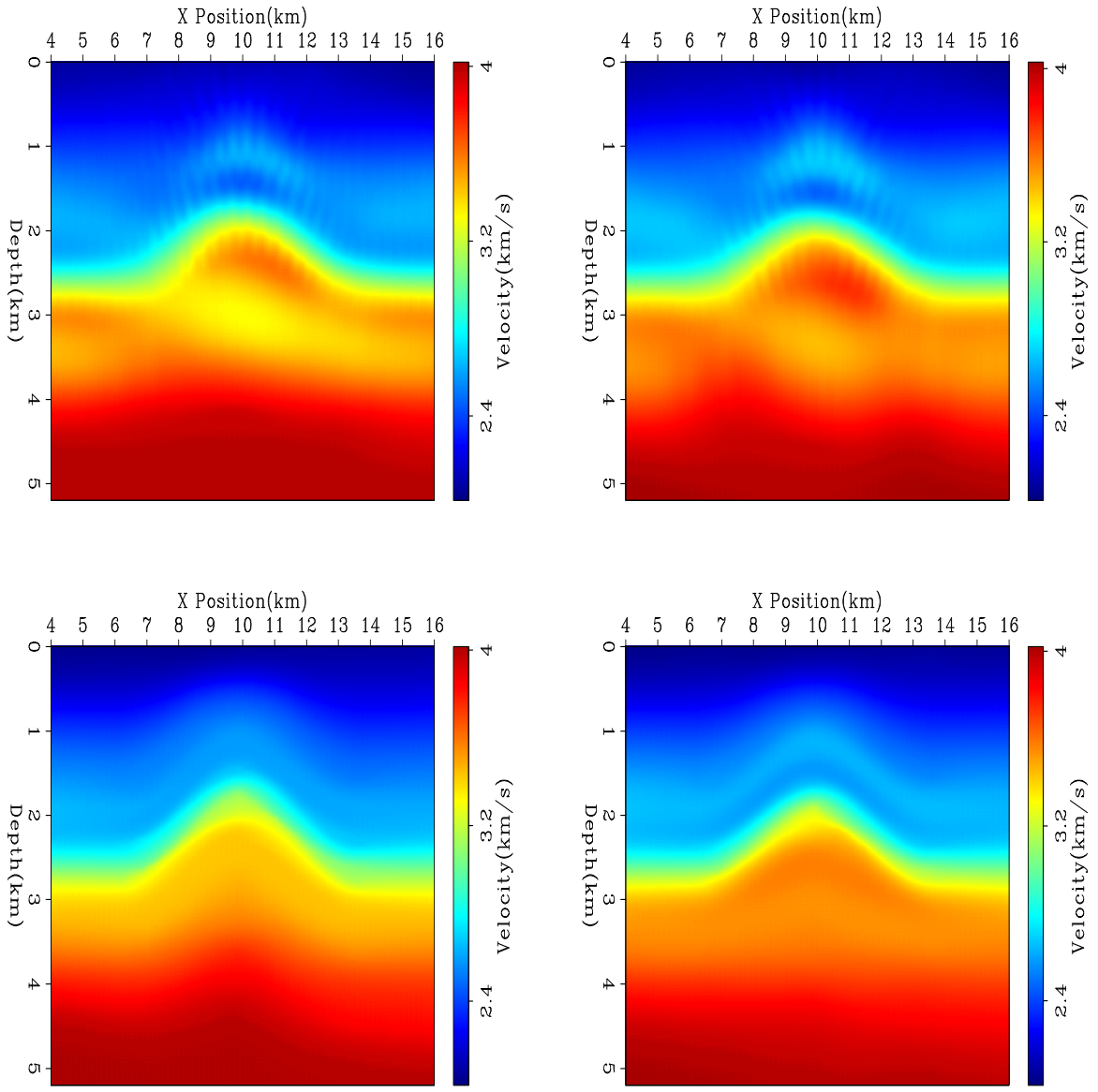

Figure 1.23: The velocity after one iteration using the four different methods. Top-left is *depth-laplacian*; top-right is *tau-laplacian*; bottom-left *depth-steering*; and bottom-right *tau-steering*. steer-anti-vel1 [ER,M]

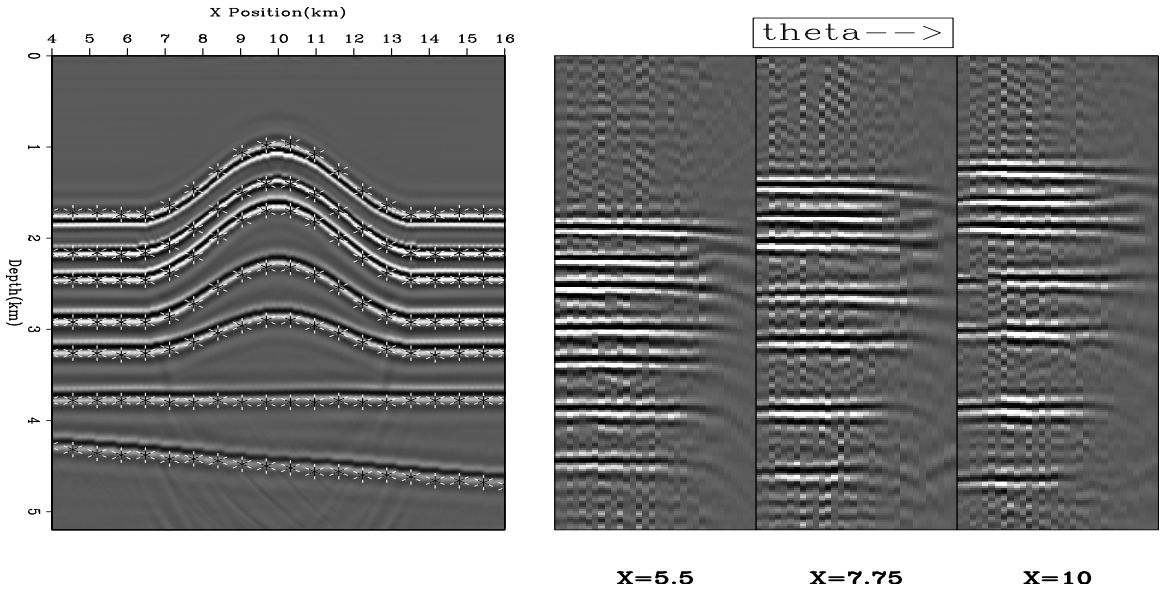

Figure 1.24: The migration result after one iteration of *depth-steering* steer-res.vel1.steerz [ER,M]

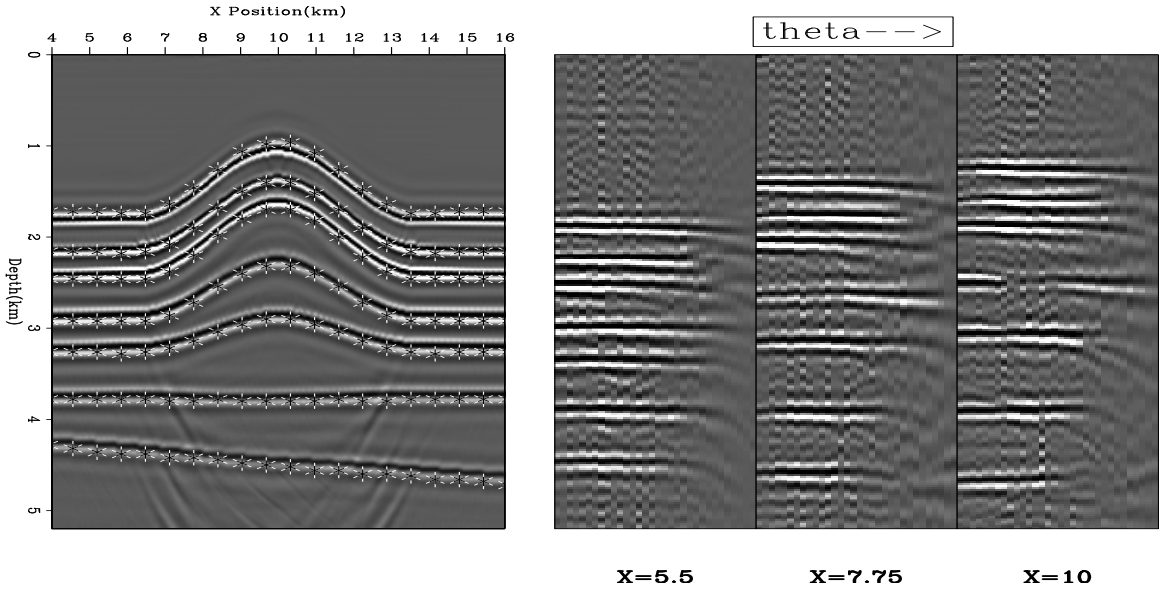

Figure 1.25: The migration result after one iteration of *tau-steering* steer-res.vel1.steer [ER,M]

Bibliography

Brown, M., 1998, Horizon refinement by synthesis of seismic and well log data: SEP–**97**, 193–206.

Carrion, P., 1991, Dual tomography for imaging complex structures: Geophysics, **56**, no. 9, 1395–1404.

Claerbout, J. Fundamentals of Geophysical Data Processing:. http://sepwww.stanford.edu/sep/prof/, 1976.

Claerbout, J. F., 1990, Nonlinear problems: SEP–**65**, 229–240.

Claerbout, J. F., 1992a, Earth Soundings Analysis: Processing versus Inversion: Blackwell Scientific Publications.

Claerbout, J. F., 1992b, Nonstationarity and conjugacy: Utilities for data patch work: SEP–**73**, 391–400.

Claerbout, J. Geophysical Estimation by Example: Environmental soundings image enhancement:. http://sepwww.stanford.edu/sep/prof/, 1998.

Claerbout, J. F., 1998b, Multi-dimensional recursive filtering via the helix: Geophysics, **63**, no. 5, 1532–1541.

Crawley, S., 1998, Shot interpolation for Radon multiple suppression: 68th Ann. Internat. Meeting, Soc. Expl. Geophys., Expanded Abstracts, 1238–1241.

Delprat-Jannaud, F., and Lailly, P., 1992, What information on the earth model do reflection travel times provide?: J. Geophysical Research, **97**, 19827–19844.

Fomel, S., and Claerbout, J. F., 1997, Exploring three-dimensional implicit wavefield extrapolation with the helix transform: SEP–**95**, 43–60.

Fomel, S., Clapp, R., and Claerbout, J., 1997, Missing data interpolation by recursive filter preconditioning: SEP–**95**, 15–25.

Harlan, W. S., 1995, Regularization by model reparameterization: http://www.billharlan.com/pub/papers/regularization.pdf.

Harlan, W. S., 1996, Promising research topics: http://sepwww.stanford.edu/oldsep/harlan/papers/seg96review

Hirsche, K., Porter-Hirsche, J., Mewhort, L., and Davis, R., 1997, The use and abuse of geostatistics: The Leading Edge, **16**, no. 03, 253–260.

Isaaks, E. H., and Srivastava, R. M., 1989, An Introduction to Applied Geostatistics: Oxford University Press.

Ji, J., 1997, Tomographic velocity estimation with plane-wave synthesis: Geophysics, **62**, no. 6, 1825–1838.

Kaipio, J. P., Kolehmainen, V., Vauhkonen, M., and Somersalo, E., 1999, Inverse problems with structural priorir information: Inverse Problems, **15**, 713–729.

Kosloff, D., Sherwood, J., Koren, Z., Machet, E., and Falkovitz, Y., 1996, Velocity and interface depth determination by tomography of depth migrated gathers: 61, **5**, no. 1511-1523.

Michelena, R. J., and Harris, J. M., 1991, Tomographic traveltime inversion using natural pixels: Geophysics, **56**, no. 5, 635–653.

Polak, E., 1997, Optimization: Algorithms and consistent approximations: Springer-Verlag, New York.

Rowbotham, P. S., and Pratt, R. G., 1997, Improved inversion through use of the null space: Geophysics, **62**, no. 3, 869–883.

Stork, C., 1994, Demonstration of mva tomography with controls and constraints for determining an accurate velocity model for prestack depth migration: 64th Annual Internat. Mtg., Soc. Expl. Geophys., Expanded Abstracts, 1338–1342.

Tarantola, A., 1987, Inverse problem theory: Elsevier.

Tikhonov, A. N., and Arsenin, V. Y., 1977, Solution of ill-posed problems: John Wiley and Sons.

van Trier, J., 1990, Tomographic determination of structural velocities from depth migrated seismic data: Ph.D. thesis, Stanford University.